information than the dominant products, since such minor products are not formed in exothermic bimolecular processes.

While such possible complications should be expected, the results of CA[8c] of $[CoRCN]^+$ ions are very similar to the chemistry presented here. There are, of course, differences in product distributions and in the observation of the least abundant products; however, the correlations are substantial. For example, no reaction products were observed for Co^+ with CH_3CN and C_2H_5CN, and there was no evidence for chemistry between these species in the analogous CA experiments. In the case of C_3H_7CN, loss of C_2H_4 is observed in both experiments; however, no loss of H_2 was observed in the ICR experiments. In the larger nitriles such as $C_6H_{13}CN$ and $C_7H_{15}CN$, it is interesting to note that loss of methane is reported from the CA experiments, but not in the ICR experiments. There are many reasons why this may occur. The ICR experiment may be less sensitive in detecting minor products. Also, the reaction may be slightly endothermic—but sufficient energy is available in the collisional activation to allow it to occur. However, since the CA results parallel the ion/molecule reaction results presented here, ions of the type $[CoRCN]^+$ formed by ligand substitution processes are apparently simple adduct ions, with the RCN still intact to a great extent.

IV. Conclusions

The –CN group appears to have unique directing abilities in the reactions of transition-metal ions with alkyl nitriles. An end-on geometry of the initially formed complex appears to explain at least some of the reactivity that follows, in which atoms of the alkyl chain far from the functional group are involved. When a CO is attached to the metal ion, the reactivity appears to change dramatically. This may be due to steric interactions at a number of points along the reaction coordinate. Before the "reactivity" of MCO^+ with alkyl cyanides can be evaluated, further work must be undertaken to determine the structure(s) of the various $MRCN^+$ product ions.

Registry No. CH_3CN, 75-05-8; C_2H_5CN, 107-12-0; C_3H_7CN, 109-74-0; C_4H_9CN, 110-59-8; $C_5H_{11}CN$, 628-73-9; $C_6H_{13}CN$, 629-08-3; $C_7H_{15}CN$, 124-12-9; $C_8H_{17}CN$, 2243-27-8; Fe^+, 14067-02-8; Co^+, 16610-75-6; Ni^+, 14903-34-5; Mn^+, 14127-69-6; Cr^+, 14067-03-9; $FeCO^+$, 35038-14-3; $CoCO^+$, 28963-35-1; $NiCO^+$, 71837-05-3; $NiPF_3^+$, 115512-35-1; $MnCO^+$, 115512-36-2; $CrCO^+$, 75474-48-5.

Synthesis of an Unstable Vinyl-Substituted Diiron–μ-Alkenyl Complex. Iron–Iron Bond Cleavage and Rearrangement to an Iron-Substituted Butadiene–Iron Complex

Charles P. Casey,* Mark S. Konings, Mark A. Gohdes, and Mark W. Meszaros

Department of Chemistry, University of Wisconsin, Madison, Wisconsin 53706

Received November 19, 1987

Reaction of diiron–μ-alkylidene complex $[C_5H_5(CO)Fe]_2(\mu\text{-}CO)(\mu\text{-}CHCH_2CH{=}CH_2)$ (1) with $(C_6H_5)_3C^+PF_6^-$ led to cleavage of the iron–iron bond and formation of $[C_5H_5(CO)Fe]\{\eta^4\text{-}1\text{-}[C_5H_5(CO)_2Fe]\text{-buta-1,3-diene}\}^+PF_6^-$ (**3PF₆**) in 86% yield by abstraction of a β-hydride and rearrangement of an intermediate μ-alkenyl complex, $[C_5H_5(CO)Fe]_2(\mu\text{-}CO)(\mu\text{-}\eta^1,\eta^2\text{-}(E)\text{-}CH{=}CHCH{=}CH_2)^+PF_6^-$ (**2PF₆**). The related tetraphenylborate salt **3BPh₄** was characterized by single-crystal X-ray crystallography: monoclinic, $P2_1/n$, $a = 9.876$ (2) Å, $b = 25.703$ (6) Å, $c = 13.155$ (3) Å, $\beta = 90.16$ (2)°, and $Z = 4$. A similar 4-phenyl-substituted butadiene-iron complex, $[C_5H_5(CO)Fe]\{\eta^4\text{-}1\text{-}[C_5H_5(CO)_2Fe]\text{-4-phenylbuta-1,3-diene}\}^+BF_4^-$ (**12BF₄**), was synthesized by condensation of phenylacetaldehyde with diiron–μ-ethylidyne complex $[C_5H_5(CO)Fe]_2(\mu\text{-}CO)(\mu\text{-}CCH_3)^+BF_4^-$ (**10**) followed by two rearrangements. **12BPh₄** was shown to be in equilibrium with rearrangement intermediate μ-alkenyl complex $[C_5H_5(CO)Fe]_2(\mu\text{-}CO)(\mu\text{-}\eta^1,\eta^2\text{-}(E,E)\text{-}CH{=}CHCH{=}CHC_6H_5)^+B(C_6H_5)_4^-$ (**11BPh₄**).

In the course of our investigations on the extensive chemistry of hydrocarbyl-bridged diiron systems $[C_5H_5(CO)Fe]_2(\mu\text{-}CO)(\mu\text{-}CR)$, we reacted diiron–μ-alkylidene complex $[C_5H_5(CO)Fe]_2(\mu\text{-}CO)(\mu\text{-}CHCH_2CH{=}CH_2)$ (1)[1] with $(C_6H_5)_3C^+PF_6^-$. We anticipated that β-hydride abstraction would occur to give vinyl-substituted μ-alkenyl-diiron complex $[C_5H_5(CO)Fe]_2(\mu\text{-}CO)(\mu\text{-}\eta^1,\eta^2\text{-}(E)\text{-}CH{=}CHCH{=}CH_2)^+PF_6^-$ (**2PF₆**) since Knox,[2] Pettit,[3] and we[4] had prepared diiron–μ-alkenyl complexes by β-hydride abstraction from μ-alkylidene complexes. Other methods are also available for the preparation of μ-alkenyl complexes.[4-6]

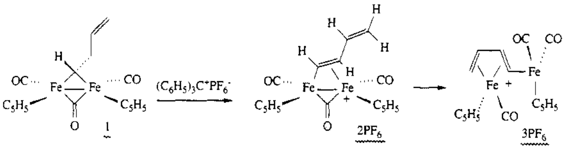

When a solution of 1 was stirred with $(C_6H_5)_3C^+PF_6^-$ in CH_2Cl_2, a bright orange crystalline compound **3PF₆** precipitated from solution over 2 h. ^1H NMR and IR spectroscopy indicated that this new material was not the expected μ-alkenyl complex **2PF₆**. No bridging carbonyl stretch was observed in the IR; only terminal carbonyl

---

[1] Casey, C. P.; Ghodes, M. A.; Meszaros, M. W. *Organometallics* **1986**, *5*, 196.

[2] Dyke, A. F.; Knox, S. A. R.; Naish, P. J.; Orpen, A. G. *J. Chem. Soc., Chem. Commun.* **1980**, 441.

[3] Kao, S. C.; Lu, P. P. Y.; Pettit, R. *Organometallics* **1982**, *1*, 411.

[4] Casey, C. P.; Marder, S. R.; Adams, B. R. *J. Am. Chem. Soc.* **1985**, *107*, 7700.

[5] Dyke, A. F.; Knox, S. A. R.; Morris, M. J.; Naish, P. J. *J. Chem. Soc., Dalton Trans.* **1983**, 1417.

[6] (a) Casey, C. P.; Meszaros, M. W.; Fagan, P. J.; Bly, R. K.; Colborn, R. E. *J. Am. Chem. Soc.* **1986**, *108*, 4053. (b) Casey, C. P.; Meszaros, M. W.; Marder, S. R.; Bly, R. K.; Fagan, P. J. *Organometallics* **1986**, *5*, 1873. (c) Casey, C. P.; Meszaros, M. W.; Colborn, R. E.; Roddick, D. M.; Miles, W. H.; Ghodes, M. A. *Organometallics* **1986**, *5*, 1879.

0276-7333/88/2307-2103$01.50/0

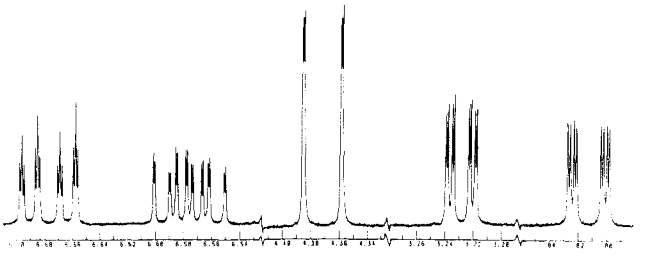

Figure 1. 500-MHz ^{1}H NMR spectrum of the vinyl hydrogens of **3PF$_6$**.

stretches were seen at 2035 (vs), 2013 (s), and 1982 (m) cm^{-1} in CH_2Cl_2 solution. No resonance for a μ-CH proton was observed near δ 12 in the ^{1}H NMR spectrum. Evidence for an intact CH=CHCH=CH$_2$ fragment was supported by ^{1}H NMR with resonances at δ 6.68 (ddt, J = 13.5, 5.6, 0.8 Hz, CH=C*H*), 6.58 (dddd, J = 11.6, 8.0, 5.6, 0.6 Hz, μ-CH=CHC*H*), 4.37 (dd, J = 13.5, 0.5 Hz, C*H*=CH), 3.23 (ddd, J = 8.0, 2.2, 0.7 Hz, CH=CHCH=C*H*H), and 0.81 (ddd, J = 11.7, 2.2, 0.9 Hz, CH=CHCH=CH*H*) (Figure 1). The high-field position of the terminal vinyl resonances is consistent with the presence of a coordinated double bond, but full spectral characterization including ^{1}H–^{13}C correlated NMR spectroscopy did not establish the structure.

Structure of $[C_5H_5(CO)Fe]\{\eta^4$-1-$[C_5H_5(CO)_2Fe]$-buta-1,3-diene$\}^+B(C_6H_5)_4^-$ (3BPh$_4$). For determination of the molecular structure of **3**, the tetraphenylborate salt **3BPh$_4$**[7] was analyzed by X-ray crystallography. In the cation of **3BPh$_4$** (Figure 2), a Cp(CO)$_2$Fe unit is σ-bonded to the buta-1,3-diene fragment and a Cp(CO)Fe unit is π-bonded in an η^4 manner to the diene as in **IIIa**. The long Fe(1)–Fe(2) distance of 3.824 Å precludes any direct iron–iron interaction. Close examination of the structure indicates that a significant but minor contribution from a second resonance structure **IIIb** is necessary to explain certain metrical parameters which deviate significantly from those expected for the simple η^4-diene formulation **IIIa**. The parameters that most noticeably support a contribution from **IIIb** are bond lengths involving the butadiene fragment. The C(1)–C(2) bond length of 1.393 (5) Å is significantly longer than the C(3)–C(4) bond length of 1.371 (6) Å, and both are longer than expected for carbon–carbon double bonds. The C(2)–C(3) bond length of 1.445 (5) Å is significantly shorter than expected for an sp^2–sp^2 hybridized carbon–carbon single bond. The short Fe(1)–C(1) bond length of 1.963 (3) Å also points to a contribution from **IIIb**. This bond length is significantly shorter than Fe–C(sp^3) bond lengths observed in a variety of Cp(CO)$_2$Fe–alkyl complexes (2.06–2.11 Å), shorter than most Fe–C(sp^2) bond lengths observed in Cp(CO)$_2$Fe–vinyl complexes (1.94–2.03 Å), and even shorter than the Fe=C bond lengths observed for some cationic Cp(CO)$_2$Fe–carbene complexes (1.91–2.00 Å).[8]

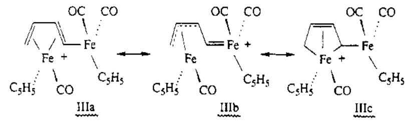

The most striking manifestation of resonance contributor **IIIb** is in the Fe(2)–C bond lengths of the coordinated butadiene. The Fe(2)–C(1) bond length of 2.338 (3) Å is 0.206–0.282 Å longer than the other Fe(2)–butadiene bond lengths: Fe(2)–C(2), 2.086 (3) Å; Fe(2)–C(3), 2.051 (3) Å; Fe(2)–C(4), 2.132 (4) Å. This is consistent with a contribution from **IIIb** in which Fe(2) and C(1) have no direct interaction and is also evidence against a contribution from a σ, σ, π interaction as in **IIIc** which could explain the observed reduction in carbon–carbon bond length alternation. This type of interaction is important in iron(0)–diene complexes where nearly equal carbon–carbon bond lengths within the butadiene fragment are observed.[9] An interaction similar to that illustrated in **IIIc** was found to be unimportant in the only other structurally characterized Cp(CO)Fe–butadiene cation we are aware of.[10]

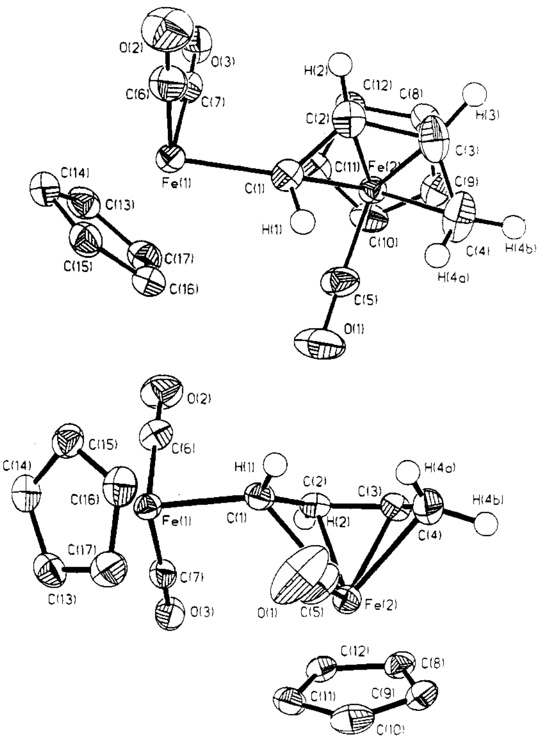

Figure 2. Structure of **3BPh$_4$**, tetraphenylborate and cyclopentadienyl hydrogens omitted for clarity. All non-hydrogen atoms are shown at the 50% probability level. Hydrogen atoms on the diene are shown as small spheres of arbitrary radius.

The orientation of the Cp(CO)$_2$Fe fragment relative to the butadiene ligand also suggests the importance of resonance structure **IIIb**. Hoffmann's theoretical study of cationic Cp(CO)$_2$Fe–carbene complexes predicted that the geometry shown in **4**, in which the plane defined by the iron atom and the carbene ligand coincides with the symmetry plane of the molecule should be favored over **5**.[11]

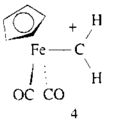

4

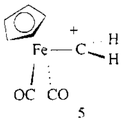

5

In 4, the d orbital not involved in back-bonding to the carbonyl groups is available for back-bonding to the carbene ligand. The geometry about Fe(1)–C(1) in **3BPh$_4$** is similar to that of **4**. The carbons of the two carbonyl groups on Fe(1) are oriented 1.21 Å above and below the mean plane defined by Fe(1) and the four carbons of the

---

[7] ^{1}H NMR spectroscopy indicated that the identity of the anion did not affect the structure of the cation.

[8] O'Connor, E. J.; Helquist, P. *J. Am. Chem. Soc.* **1982**, *104*, 1869 and references contained therein.

[9] Cotton, F. A.; Day, V. W.; Frenz, B. A.; Hardcastle, K. I.; Troup, J. M. *J. Am. Chem. Soc.* **1973**, *95*, 4522.

[10] Lee, Q.-H.; Peng, S.-M.; Lush, S.-F.; Liao, M.-Y.; Liu, R.-S. *Organometallics* **1987**, *6*, 2094.

[11] Schiller, B. E. R.; Hoffmann, R.; Lichtenberger, D. L. *J. Am. Chem. Soc.* **1979**, *101*, 585.

butadiene unit. This is the geometry that would be predicted on the basis of the carbene-like nature of C(1) as suggested in resonance structure **IIIb**.

Infrared spectroscopy also supports a description of **$3PF_6$** with a minor contribution from resonance structure **IIIb**. We assign bands at 2035 (vs) and 1982 (m) cm^{-1} to symmetric and antisymmetric terminal carbonyl stretches of the $Cp(CO)_2Fe$ fragment and the band at 2013 (s) cm^{-1} to the terminal carbonyl stretch of the Cp(CO)Fe unit. The 53 cm^{-1} separation between the bands assigned to the symmetric and antisymmetric carbonyl stretches of the $Cp(CO)_2Fe$ fragment of **$3PF_6$** is similar to the 43–54 cm^{-1} separation seen for other $Cp(CO)_2Fe$ complexes (Table III, entries 1–8). The $Cp(CO)_2Fe$ bands of **$3PF_6$** appear at higher frequency than those of most other $Cp(CO)_2Fe$–vinyl complexes (entries 1, 2, 4). Only the complex in entry 3, with an electron-withdrawing carbethoxy substituent on the vinyl group, has high-energy stretches similar to that seen for **$3PF_6$**. These results indicate decreased electron density on Fe(1) of **$3PF_6$** as suggested by resonance structure **IIIb**. The $Cp(CO)_2Fe$–carbonyl stretches for **$3PF_6$** are lower in energy than observed for cationic $Cp(CO)_2Fe$–carbene complexes (entries 5–8); this is an indication that resonance structure **IIIb** is a minor contributor to the structure of **$3PF_6$**.

The carbonyl stretch of the Cp(CO)Fe fragment in **$3PF_6$**, 2013 (s) cm^{-1}, is lower in energy than other cationic Cp(CO)Fe–diene complexes (entries 9–12) and shows that a $Cp(CO)_2Fe$ substituent on the butadiene ligand is able to substantially increase the electron density at Fe(2).

Rearrangement of Vinyl-Substituted μ-Alkenyl Complexes to η^4-Buta-1,3-diene Complexes. When the reaction between alkylidene complex **1** (0.05 M) and $(C_6H_5)_3C^+PF_6^-$ (0.05 M) in CD_2Cl_2 at −3 °C was monitored by ^1H NMR with hexamethylbenzene as an internal standard, an intermediate with resonances consistent with μ-alkenyl complex **$2PF_6$** was observed. Resonances at δ 11.99 (d, $J = 11.2$ Hz) for the μ-CH proton and δ 4.23 (t, $J = 11.6$ Hz) for the μ-CH=C*H* proton were crucial in helping to establish the structure of this intermediate as **$2PF_6$**. In addition, two vinyl resonances were observed at δ 5.65 (d, $J = 14.5$ Hz, μ-CH=CHCH=C*H*H) and 5.49 (d, $J = 10.4$ Hz, μ-CH=CHCH=CH*H*). The remaining vinyl proton and the Cp protons were obscured by CD_2Cl_2 solvent (δ 5.32). At −3 °C, the conversion of μ-alkenyl complex **$2PF_6$** to butadiene complex **$3PF_6$** is slow. After 65 min at −3 °C, the ratio of **$2PF_6$:$3PF_6$** was 4.9:1.0 (94% yield). **$2PF_6$** quickly rearranged to **$3PF_6$** upon warming to ambient temperature (**$2PF_6$:$3PF_6$**, 1.0:1.0 after 10 min; **$2PF_6$:$3PF_6$**, 1.0:2.0 after 20 min). After 45 min at ambient temperature, only resonances for **$3PF_6$** were observed (92%).

δ,δ-Disubstituted μ-dienyl complexes **6**, **7**, and **8** do not rearrange to butadiene complexes similar to **3**. Vinyl-substituted μ-alkenyl complex **6** was obtained previously as one product of the reaction of diiron–μ-methylidyne complex $[C_5H_5(CO)Fe]_2(\mu\text{-}CO)(\mu\text{-}CH)^+PF_6^-$ (**9**) with 3,3-dimethyl-1-butyne.[19] μ-Alkenyl complexes **7** and **8** were prepared by the condensation of diiron–μ-ethylidyne complex $[C_5H_5(CO)Fe]_2(\mu\text{-}CO)(\mu\text{-}CCH_3)^+BF_4^-$ (**10**) with isobutyraldehyde and cyclohexanecarboxaldehyde.[20] The fact that none of these compounds having two alkyl substituents at the terminal vinyl carbon rearranged to a butadiene complex suggests that steric factors destabilize η^4-butadiene coordination.

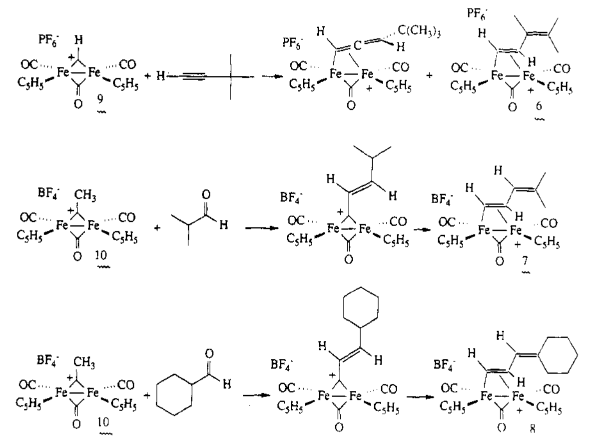

To probe the steric requirements for η^4-butadiene coordination, we studied the reaction between ethylidyne complex **10** and phenylacetaldehyde. **10** reacts with a variety of aldehydes, ketones, and orthoesters to give vinyl carbyne complexes.[20] Vinyl carbyne complexes generated by condensation of enolizable aldehydes with **10** are unstable under the reaction conditions, and, for selected aldehydes, rearrangements to vinyl-substituted μ-alkenyl complexes are observed. Ethylidyne complex **10** reacted with phenylacetaldehyde in CH_2Cl_2 at 40 °C over 4 h. Crystallization from CH_2Cl_2–diethyl ether gave an orange-brown powder which was shown by ^1H NMR to be a 1.6:1.0 mixture of μ-alkenyl complex $[C_5H_5(CO)Fe]_2(\mu\text{-}CO)(\mu\text{-}\eta^1,\eta^2\text{-}(E,E)\text{-}CH{=}CHCH{=}CHC_6H_5)^+BF_4^-$ (**$11BF_4$**) and butadiene complex $[C_5H_5(CO)Fe]\{\eta^4\text{-}1\text{-}[C_5H_5(CO)_2Fe]\text{-}4\text{-phenylbuta-1,3-diene}\}^+BF_4^-$ (**$12BF_4$**). In the

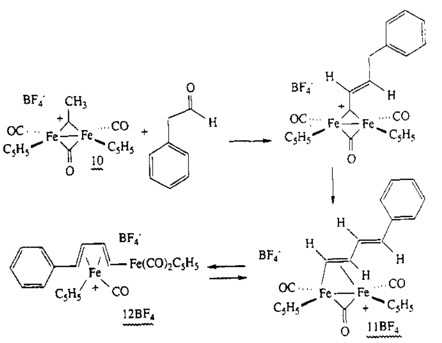

500-MHz ^1H NMR spectrum seven of the eight vinyl resonances were observed as well-resolved multiplets. Complete connectivities and the presence of the eighth vinyl resonance were established by decoupling experiments. Conversion of the BF_4^- salts into the corresponding $B(C_6H_5)_4^-$ salts and vapor diffusion of diethyl ether into a solution of **11** and **12** in CH_2Cl_2 at 25 °C gave a purple-brown crystalline material. When this material was dissolved in acetone-d_6 at −40 °C and placed in a precooled NMR probe at −20 °C, only resonances for μ-alkenyl

---

(12) Casey, C. P.; Marder, S. R.; Colborn, E. E.; Goodson, P. A. *Organometallics* **1986**, *5*, 199.

(13) Casey, C. P.; Austin, E. A.; Rheingold, A. L. *Organometallics* **1987**, *6*, 2157.

(14) Churchill, M. R.; Wormald, J.; Biering, W. P.; Emerson, G. F. *J. Chem. Soc., Chem. Commun.* **1968**, 1217.

(15) Casey, C. P.; Miles, W. H.; Tukada, H. *J. Am. Chem. Soc.* **1985**, *107*, 2924.

(16) Allison, N. T.; Kawada, Y.; Jones, W. M. *J. Am. Chem. Soc.* **1978**, *100*, 5224.

(17) Priester, W.; Rosenblum, M. *J. Chem. Soc., Chem. Commun.* **1978**, 26.

(18) Giulieri, F.; Benaim, J. *J. Organomet. Chem.* **1984**, *276*, 367.

(19) Casey, C. P.; Woo, L. K.; Fagan, P. J.; Palermo, R. E.; Adams, B. R. *Organometallics* **1987**, *6*, 447.

(20) Casey, C. P.; Konings, M. S.; Marder, S. R. *Polyhedron*, in press.

Table I. Selected Bond Lengths and Bond Angles for 3BPh$_4$

	Bond Lengths (Å)		
Fe(1)–C(1)	1.963 (3)	C(7)–O(3)	1.138 (4)
Fe(1)–C(7)	1.762 (3)	Fe(1)–C(6)	1.767 (3)
Fe(2)–C(1)	2.338 (3)	Fe(2)–C(2)	2.086 (3)
Fe(2)–C(3)	2.051 (4)	Fe(2)–C(4)	2.132 (4)
Fe(2)–C(5)	1.766 (4)	C(1)–C(2)	1.393 (5)
C(1)–H(1)	0.958 (32)	C(2)–C(3)	1.445 (5)
C(2)–H(2)	0.967 (30)	C(3)–C(4)	1.371 (6)
C(3)–H(3)	1.024 (40)	C(4)–H(4b)	1.016 (35)
C(4)–H(4a)	0.931 (38)	C(6)–O(2)	1.140 (4)
C(5)–O(1)	1.139 (5)		
	Bond Angles (deg)		
Fe(1)–C(1)–H(1)	114.7 (21)	C(1)–C(2)–H(2)	124.5 (19)
Fe(1)–C(1)–C(2)	127.9 (2)	C(1)–C(2)–C(3)	124.0 (3)
H(1)–C(1)–C(2)	113.9 (21)	C(2)–C(3)–H(3)	119.3 (22)
H(2)–C(2)–C(3)	110.8 (19)	C(2)–C(3)–C(4)	120.8 (3)
H(3)–C(3)–C(4)	119.7 (22)	C(3)–C(4)–H(4a)	119.7 (26)
H(4a)–C(4)–H(4b)	118.3 (34)	C(3)–C(4)–H(4b)	117.3 (24)

Table II. Summary of Crystal Data and Intensity Collection for 3BPh$_4$

empirical formula	$C_{41}H_{35}BFe_2O_3$
fw	698.223
cryst dimensn, mm	0.50 × 0.45 × 0.35
temp, K	160
cell parameters	
a, Å	9.876 (2)
b, Å	25.703 (6)
c, Å	13.155 (3)
β, deg	90.16 (2)
space group	$P2_1/n$
Z	4
d(calcd), g/cm^3	1.39
absorptn coeff μ, cm^{-1}	9.05
Nicolet diffractometer[a]	$P\bar{1}$
scan type	Wycoff
scan range, deg	0.1
background offset	1.0
scan speed, deg min^{-1}	3.5–29.3
Bkgd/scan ratio	1.00
2θ limits, deg	3.50–58.70
max $(\sin\theta)/\lambda$, Å^{-1}	0.690
absorptn correctn	none
unique data, theoretical	9175
$F_o > 3\sigma(F_o)$	6869
p; weight = $[\sigma^2(F) + p^2F^2]^{-1}$	0.0008
discrepancy indices	
R, %	5.89
R_w, %	5.80
goodness of fit	1.39
observn/variable ratio	15.5
final difference ρ_{max}, e/Å^3	0.63

[a] Diffractometer equipped with a graphite-monochromated Mo Kα radiation source.

complex **11BPh$_4$** were observed. At 0 °C, resonances for butadiene complex **12BPh$_4$** appeared and then increased in intensity upon further warming. After 15 min at 25 °C, a 1.3:1.0 equilibrium ratio of complexes **11BPh$_4$/12BPh$_4$** was reached. Cooling the sample to −40 °C did not change the ratio of **11BPh$_4$/12BPh$_4$**. These results provide definite evidence for an equilibrium between μ-alkenyl complex **11** and butadiene complex **12**.

Summary. The rearrangement of μ-η^1,η^2-dienyl compounds with iron–iron bonds to iron-substituted η^4-dienyl compounds without iron–iron bonds is evidently a facile and reversible process. With no carbon substituents on the terminal carbon of the dienyl unit, rearrangement of **2** to **3** proceeded to completion. With a single carbon substituent on the terminal dienyl carbon, an equilibrium between the two structural types (**11BPh$_4$** and **12BPh$_4$**) was established. With two substituents on the terminal dienyl carbon, no rearrangement was seen presumably because the potential η^4-dienyl complex is greatly destabilized by steric hindrance.

Experimental Section

General Data. ^{1}H NMR spectra were obtained on a Bruker WP270 or AM500 spectrometer. ^{13}C NMR spectra of samples containing 0.07 M Cr(acac)$_3$ as a shiftless relaxation agent were obtained on a AM500 spectrometer operating at 126 MHz. Infrared spectra were obtained on a Mattson Polaris FTIR spectrometer. Acetone-d_6 was dried over B_2O_3. CD_2Cl_2 was dried over P_2O_5. CH_2Cl_2 was distilled from CaH_2 twice prior to use. Diethyl ether, hexane, and THF were distilled from purple solutions of sodium and benzophenone immediately prior to use. $Na^+B(C_6H_5)_4^-$ was dried at 110 °C under vacuum prior to use.

$[C_5H_5(CO)Fe]\{\eta^4$-1-$[C_5H_5(CO)_2Fe]$-buta-1,3-diene$\}^+PF_6^-$ (3PF$_6$). **1**[1] (165 mg, 0.434 mmol) and $(C_6H_5)_3C^+PF_6^-$ (160 mg, 0.412 mmol) were stirred in CH_2Cl_2 (20 mL) at 0 °C for 1 h and then at 15 °C for 40 min. The volume of solvent was reduced to 2 mL by evaporation under high vacuum, and hexane (10 mL) was condensed in at −78 °C. A bright orange crystalline material was collected by filtration on a reversible Schlenk filter frit, washed twice with diethyl ether (2 mL), and dried under vacuum to give pure **3PF$_6$** (186 mg, 86%). ^{1}H NMR (acetone-d_6, 500 MHz): δ 6.68 (ddt, J = 13.5, 5.6, 0.8 Hz, μ-CH═C*H*), 6.58 (dddd, J = 11.6, 8.0, 5.6, 0.6 Hz, μ-CH═CHC*H*), 5.43 (s, C_5H_5), 5.36 (s, C_5H_5), 4.37 (dd, J = 13.5, 0.5 Hz, μ-CH), 3.23 (ddd, J = 8.0, 2.2, 0.7 Hz, μ-CH═CHCH═C*H*H), 0.81 (ddd, J = 11.7, 2.2, 0.9 Hz, μ-CH═CHCH═CH*H*). ^{13}C NMR (acetone-d_6): δ 221.2, 215.0, 214.3 (CO); 126.5 (d, J = 149 Hz, μ-CH); 98.3 (d, J = 168 Hz, μ-CH═*C*H); 88.4, 84.7 (C_5H_5); 83.9 (μ-CH═CH*C*H); 46.4 (CH_2). Assignments are based on 2D ^{1}H–^{13}C correlated NMR. IR (CH_2Cl_2): 2035 (vs), 2013 (s), 1982 (m) cm^{-1}. Anal. Calcd for $C_{17}H_{15}F_6Fe_2O_3P$: C, 38.97; H, 2.89. Found: C, 38.70; H, 2.94.

$[C_5H_5(CO)Fe]\{\eta^4$-1-$[C_5H_5(CO)_2Fe]$-buta-1,3-diene$\}^+B(C_6H_5)_4^-$ (3BPh$_4$). **3PF$_6$** (44 mg, 0.084 mmol) and $Na^+B(C_6H_5)_4^-$ (975 mg, 2.85 mmol) were stirred in CH_2Cl_2 (15 mL) for 1 h at ambient temperature and filtered. The volume of solvent was reduced to 2 mL, and diethyl ether (10 mL) was condensed in to give a bright orange crystalline material. This material was washed with 2 mL of solvent and dried under vacuum to give pure **3BPh$_4$** (46

Table III. Carbonyl Stretching Frequencies of Cp(CO)$_2$Fe–Vinyl, Cationic Cp(CO)$_2$Fe–Carbene, and Cationic Cp(CO)Fe–Butadiene Complexes

entry	compound	IR (cm^{-1})	ref
1	$Cp(CO)_2FeCH{=}CH_2$	2011 (s), 1957 (s)	12
2	$Cp(CO)_2FeCH{=}CHCH_2CH_2CH_3$	2007 (s), 1960 (s)	12
3	$Cp(CO)_2FeCH{=}CHCO_2CH_2CH_3$	2028 (s), 1982 (vs)	13
4	$Cp(CO)_2FeCH{=}CHCH{=}CHFe(CO)_2Cp$	2000, 1950[a]	14
5	$Cp(CO)_2Fe{=}C(CH_3)_2^+BF_4^-$	2076 (s), 2031 (s)	15
6	$Cp(CO)_2Fe{=}CHCH{=}C(CH_3)_2^+BF_4^-$	2065 (s), 2022 (s)	15
7	$Cp(CO)_2Fe{=}C(CH_3)(OCH_3)^+BF_4^-$	2060 (s), 2014 (s)	15
8	$Cp(CO)_2Fe{=}\overline{CCH{=}CHCH{=}CHCH{=}C}H^+PF_6^-$	2045, 1996[a]	16
9	$Cp(CO)Fe(\eta^4\text{-}CH_2{=}CHCH{=}CH_2)^+BF_4^-$	2055	17
10	$Cp(CO)Fe[\eta^4\text{-}CH_2{=}C(CO_2CH_3)CH{=}C{=}CHCH_3]^+BF_4^-$	2065	18
11	$Cp(CO)Fe(\eta^4\text{-}CH_3CH{=}CHCH{=}CHCH_3)^+PF_6^-$	2028	10
12	$Cp(CO)Fe(\eta^4\text{-}CH_2{=}CHCH{=}CHCH_3)^+PF_6^-$	2030	10

[a] Intensities not given.

mg, 78%) as shown by ^{1}H NMR.

Reaction of $[C_5H_5(CO)Fe]_2(\mu\text{-}CO)(\mu\text{-}CCH_3)^+BF_4^-$ (10) with Phenylacetaldehyde. 10[21] (200 mg, 0.455 mmol) and phenylacetaldehyde (0.5 g, 4 mmol) were stirred in CH_2Cl_2 (75 mL) at 40 °C for 4 h. Solvent was evaporated under reduced pressure, and THF (2 mL) was added. The solution was filtered to remove traces of $CpFe(CO)_3^+$, and the solvent was evaporated. CH_2Cl_2 (1 mL) and then diethyl ether (25 mL) were added, and an orange-brown powder was isolated by filtration to give a 1.6:1.0 mixture of **11BF$_4$**/**12BF$_4$** (244 mg, 99%). ^{1}H NMR spectroscopy indicated this material was ~85% pure. Repeated crystallizations failed to give pure material. ^{1}H NMR (acetone-d_6, 500 MHz) of the mixture of **11BF$_4$** and **12BF$_4$**: for **11BF$_4$**, δ 12.27 (d, J = 12.4 Hz, μ-CH), 7.62 (m, 2 H, C_6H_5), 7.37 (m, 3 H, C_6H_5), 7.20 (d, J = 15.0 Hz, μ-CH=CHCH=C*H*), 7.11 (dd, J = 15.6, 9.8 Hz, μ-CH=CHC*H*), 5.67 (s, 10 H, C_5H_5), 4.69 (t, J = 11.2 Hz, μ-CH=C*H*); for **12BF$_4$**, δ 7.55 (m, 2 H, C_6H_5), 7.33 (m, 3 H, C_6H_5), 7.33 (dd, J = 11.6, 5.8 Hz, μ-CH=CHC*H*, obscured by C_6H_5, established through decoupling experiments), 6.78 (ddd, J = 13.5, 5.8, 0.7 Hz, μ-CH=C*H*), 5.38 (s, C_5H_5), 5.21 (s, C_5H_5), 4.65 (d, J = 13.4, μ-CH), 2.57 (d, J = 11.6 Hz, μ-CH=CHCH=C*H*). $^{13}C\{^1H\}$ NMR (acetone-d_6, 126 MHz) for **11BF$_4$** and **12BF$_4$**; δ 221.3, 216.6, 214.8, 211.5 (CO); 175.0, 138.2, 137.7, 137.1, 131.3, 129.9, 129.5, 129.4, 129.3, 127.9, 127.8, 124.7, 99.4, 94.7, 79.2, 72.0 (aryl and vinyl); 91.4, 88.5, 85.2 (C_5H_5) (μ-CO not observed).

$[C_5H_5(CO)Fe]_2(\mu\text{-}CO)(\mu\text{-}\eta^1,\eta^2\text{-}(E,E)\text{-}CH{=}CHCH{=}CHC_6H_5)^+B(C_6H_5)_4^-$ (11BPh$_4$). A mixture of **11BF$_4$** and **12BF$_4$** (240 mg, 0.443 mmol) and $Na^+B(C_6H_5)_4^-$ (660 mg, 1.93 mmol) were stirred in CH_2Cl_2 (5 mL) at ambient temperature for 5 min, and then the solution was filtered. The volume of solvent was reduced to 2 mL. The solution was allowed to equilibrate in a closed system containing 40 mL of diethyl ether under a pressure of 50 mmHg of N_2 for 6 h. Over this time, purple crystals precipitated from solution. The crystals were collected by filtration, washed three times with 5-mL portions of solvent, and dried under vacuum to give **12BPh$_4$** (185 mg, 54%). ^{1}H NMR spectroscopy showed several impurities (~10%). Suspension of this material in CH_2Cl_2 (1 mL) and filtration gave pure **12BPh$_4$** (105 mg, 31%). IR (CH_2Cl_2): 2034 (vs), 2009 (s), 1984 (m), 1850 (m) cm^{-1}. Despite the crystalline nature of this material, attempts to obtain fully satisfactory analysis were unsuccessful. Anal. Calcd for $C_{47}H_{39}BFe_2O_3$: C, 72.90, H, 5.08. Found: C, 72.05; H, 5.00.

X-ray Crystallography. Attempts to grow X-ray quality crystals of **3PF$_6$** gave very thin plates. Large trapezoidal blocks of **3BPh$_4$** suitable for X-ray analyses were grown by diffusion of diethyl ether into a concentrated solution of **3BPh$_4$** in CH_2Cl_2 at −18 °C. A summary of crystal data and intensity collection, lists of selected bond lengths and bond angles are shown in Tables I and II. Data reduction, solution, and refinement of the structure proceeded smoothly with the SHELXTL structure determination package (Nicolet XRD Corp., Madison, WI) similar to that described previously.[22] Hydrogen atoms on the butadiene fragment were located and refined isotropically and constrained to have similar C–H bond lengths. A ψ-scan absorption correction was applied but had a negligible effect and was not used.

Acknowledgment. Support from the National Science Foundation is gratefully acknowledged. M.S.K. thanks SOHIO for a fellowship. We thank Dr. Bruce R. Adams for help with the 2D NMR.

Registry No. 1, 116296-58-3; **3PF$_6$**, 116184-96-4; **3BF**, 116184-97-5; **10**, 116261-26-8; **11BF$_4$**, 116184-99-7; **11BPh$_4$**, 116261-27-9; **12BF$_4$**, 116185-01-4; **12BPh$_4$**, 116185-02-5; $(C_6H_5)_3C^+PF_6^-$, 437-17-2; $Na^+B(C_6H_4)_4^-$, 143-66-8; phenylacetaldehyde, 122-78-1.

Supplementary Material Available: A figure of the $B(C_6H_5)_4^-$ counterion and tables of atomic coordinates, bond lengths, bond angles, anisotropic thermal parameters, and hydrogen atom coordinates and thermal parameters (7 pages); a listing of observed and calculated structure factors (55 pages). Ordering information is given on any current masthead page.

---

[21] Nitay, M.; Priester, W.; Rosenblum, M. *J. Am. Chem. Soc.* **1978**, *100*, 3620.

[22] Haller, K. J.; Enemark, J. H. *Inorg. Chem.* **1978**, *17*, 3552.